



J/ψ production as a function of charged particle multiplicity in pp collisions at $\sqrt{s} = 7$ TeV[☆]

ALICE Collaboration

ARTICLE INFO

Article history:

Received 13 February 2012

Received in revised form 12 April 2012

Accepted 21 April 2012

Available online 25 April 2012

Editor: V. Metag

ABSTRACT

The ALICE Collaboration reports the measurement of the relative J/ψ yield as a function of charged particle pseudorapidity density $dN_{\text{ch}}/d\eta$ in pp collisions at $\sqrt{s} = 7$ TeV at the LHC. J/ψ particles are detected for $p_t > 0$, in the rapidity interval $|y| < 0.9$ via decay into e^+e^- , and in the interval $2.5 < y < 4.0$ via decay into $\mu^+\mu^-$ pairs. An approximately linear increase of the J/ψ yields normalized to their event average $(dN_{J/\psi}/dy)/(dN_{\text{ch}}/dy)$ with $(dN_{\text{ch}}/d\eta)/(dN_{\text{ch}}/d\eta)$ is observed in both rapidity ranges, where $dN_{\text{ch}}/d\eta$ is measured within $|\eta| < 1$ and $p_t > 0$. In the highest multiplicity interval with $\langle dN_{\text{ch}}/d\eta(\text{bin}) \rangle = 24.1$, corresponding to four times the minimum bias multiplicity density, an enhancement relative to the minimum bias J/ψ yield by a factor of about 5 at $2.5 < y < 4$ (8 at $|y| < 0.9$) is observed.

© 2012 CERN. Published by Elsevier B.V. Open access under CC BY-NC-ND license.

Understanding the production mechanism of quarkonium states in hadronic collisions is still a challenge due to its sensitivity to perturbative and non-perturbative aspects of Quantum Chromodynamics (QCD). While the primary production of heavy quark–antiquark ($q\bar{q}$) pairs is generally treated as a hard process which can be calculated within perturbative QCD, the subsequent formation of a bound colorless $q\bar{q}$ pair is inherently non-perturbative and difficult to treat. The models developed to describe quarkonium production in high energy hadron collisions consequently follow various approaches, mainly differing in the relative contribution of the intermediate color singlet and color octet $q\bar{q}$ states [1,2]. Recent theoretical work tries to describe consistently [3–5] the measured production cross section and polarization, in particular in light of recent measurements at the LHC [6–11].

It is also important to consider that a high energy proton–proton collision can have a substantial contribution from Multi-Parton Interactions (MPI) [12,13]. In this case several interactions on the parton level can occur in a single pp collision, which can introduce a dependence of particle production on the total event multiplicity [14–16]. If MPI were mainly affecting processes involving only light quarks and gluons, as implemented e.g. in PYTHIA 6.4, processes like J/ψ and open heavy flavor production should not be influenced and their rates are expected to be independent of the overall event multiplicity. However, at the high center-of-mass energies reached at the LHC, there might be a substantial contribution of MPI on a harder scale which can also induce a correlation between the yield of quarkonia and the total charged particle multiplicity [17]. An early study that relates open

charm production and underlying event properties was performed by the NA27 experiment for pp collisions at $\sqrt{s} = 27$ GeV, with the result that charged particle multiplicity distributions in events with open charm production have a mean that is higher by $\sim 20\%$ than the ones without [18].

In [19,20] it has been argued that, due to the spatial distribution of partons in the transverse plane (as described in generalized parton distributions), the density of partons in pp collisions will be strongly impact parameter dependent. Therefore, the probability for MPI to occur will increase towards smaller impact parameters. This effect might be further enhanced by quantum-mechanical fluctuations of the small Bjorken- x gluon densities.

The charged particle multiplicities measured in high-multiplicity pp collisions at LHC energies reach values that are of the same order as those measured in heavy-ion collisions at lower energies (e.g. they are well above the ones observed at RHIC for peripheral Cu–Cu collisions at $\sqrt{s_{\text{NN}}} = 200$ GeV [21]). Therefore, it is a valid question whether pp collisions also exhibit any kind of collective behavior as seen in these heavy-ion collisions. An indication for this might be the observation of long range, near-side angular correlations (ridge) in pp collisions at $\sqrt{s} = 0.9, 2.36$ and 7 TeV with charged particle multiplicities above four times the mean multiplicity [22,23]. Since quarkonium yields in heavy-ion reactions are expected to be modified relative to minimum bias pp collisions [24–26], one might ask whether their production rates in high-multiplicity pp collisions are already exhibiting any effect like J/ψ suppression.

In this Letter, we report the first measurement of relative J/ψ production yields $(dN_{J/\psi}/dy)/(dN_{\text{ch}}/dy)$ at mid-rapidity ($|y| < 0.9$) and at forward rapidity ($2.5 < y < 4$) as a function of the relative charged particle multiplicity density $(dN_{\text{ch}}/d\eta)/(dN_{\text{ch}}/d\eta)$

[☆] © CERN for the benefit of the ALICE Collaboration.

as determined in $|\eta| < 1$ for pp collisions at $\sqrt{s} = 7$ TeV at the LHC.

The data discussed here are measured in two complementary parts of the experimental setup of ALICE [27]: the central barrel ($|\eta| < 0.9$) for the J/ψ detection in the di-electron channel and the muon spectrometer ($-4 < \eta < -2.5$)¹ for $J/\psi \rightarrow \mu^+\mu^-$ measurements.

The central barrel provides momentum measurement for charged particles with $p_t > 100$ MeV/c and particle identification up to $p_t \approx 10$ GeV/c. Its detectors are all located inside a large solenoidal magnet with a field strength of 0.5 T. Used in this analysis are the Inner Tracking System (ITS) and the Time Projection Chamber (TPC). The ITS [28] consists of six layers of silicon detectors surrounding the beam pipe at radial positions between 3.9 cm and 43.0 cm. Silicon Pixel Detectors (SPD) are used for its innermost two layers and allow a precise reconstruction of the interaction vertex. The TPC [29] is a large cylindrical drift volume covering the range along the beam axis relative to the Interaction Point (IP) between $-250 < z < 250$ cm and extending in the radial direction from 85 cm to 247 cm. It is the main tracking device in the central barrel and is also used for particle identification via a measurement of the specific ionization (dE/dx) in the detector gas with a resolution of about 5% [27].

The muon spectrometer consists of a frontal absorber followed by a 3 Tm dipole magnet, coupled to tracking and triggering detectors. Muons are filtered by the 10 interaction length (λ_I) thick absorber placed between 0.9 m and 5.0 m from the nominal position of the IP along the beam axis. Muon tracking is performed by five tracking stations, positioned between 5.2 m and 14.4 m from the IP, each consisting of two planes of cathode pad chambers. The muon triggering system consists of two stations positioned at 16.1 m and 17.1 m from the IP, each equipped with two planes of resistive plate chambers. It is located downstream of a 1.2 m thick iron wall ($7.2\lambda_I$) which absorbs hadrons penetrating the frontal absorber, secondary hadrons escaping the absorber material, and low-momentum muons ($p < 4$ GeV/c). A conical absorber surrounding the beam pipe provides protection against secondary particles throughout the full length of the muon spectrometer. These particles result from interactions not associated with the primary vertex and are mainly due to beam–gas interactions.

Two VZERO detectors are used for triggering on inelastic pp interactions and for the rejection of beam–gas events. They consist of scintillator arrays and are positioned at $z = -90$ cm and $z = +340$ cm, covering the pseudorapidity ranges $-3.7 < \eta < -1.7$ and $2.8 < \eta < 5.1$. The minimum bias (MB) pp trigger uses the information of the VZERO detectors and the SPD. It is defined as the logical OR between two conditions: (i) a signal in at least one of the two VZERO detectors has been measured; (ii) at least one readout chip in the SPD fires. It has to be in coincidence with the arrival of proton bunches from both sides of the interaction region. The efficiency of the MB trigger to record inelastic collisions was evaluated by Monte Carlo studies and is 86.4% [30]. For the di-muon analysis, a more restrictive trigger is used (μ -MB). It requires the detection of at least one muon above a threshold of $p_t^{\text{trig}} > 0.5$ GeV/c in the muon trigger chambers in addition to the MB trigger requirement.

The results presented in this Letter are obtained by analyzing pp collisions at $\sqrt{s} = 7$ TeV recorded in 2010. For the J/ψ measurement in the di-electron (di-muon) channel a sample of 3.5×10^8 minimum bias events (6.75×10^6 μ -MB triggered events)

is analyzed, corresponding to an integrated luminosity of 5.6 nb^{-1} (7.7 nb^{-1}). The relative normalization between the number of μ -MB and minimum bias triggers needed to extract the integrated luminosity in the di-muon case is calculated using the ratio of the number of corresponding single muons with $p_t > 1$ GeV/c. The luminosity at the ALICE interaction point was kept between 0.6 and $2.0 \times 10^{29} \text{ cm}^{-2} \text{ s}^{-1}$ for all the data used in this analysis. This ensures a collision pile-up rate not larger than 4% in each bunch crossing. In the case of the di-muon analysis the interaction vertex is reconstructed using tracklets which are defined as combinations of two hits in the SPD layers of the ITS, one hit in the inner layer and one in the outer. Since for MB trigger used in the di-electron analysis the full information of the central barrel detectors is available (μ -MB triggered events only include SPD information), tracks measured with ITS and TPC are used in this case to locate the interaction vertex. This results in a resolution in z direction of $\sigma_z \approx 600/N_{\text{trk}}^{0.7} \mu\text{m}$, where N_{trk} is the multiplicity measured via SPD tracklets. For the vertices reconstructed using SPD tracklets only, this resolution is worse by 35% for high ($N_{\text{trk}} = 40$) and 50% for low ($N_{\text{trk}} = 10$) multiplicities. Events that do not have an interaction vertex within $|z_{\text{vtx}}| < 10$ cm are rejected, where z_{vtx} is the reconstructed z position of the vertex. The rms of the vertex distributions along z is for all running conditions below 6.6 cm and no significant dependence on $dN_{\text{ch}}/d\eta$ is found for the multiplicity intervals studied here.

Pile-up events are identified by the presence of two interaction vertices reconstructed with the SPD. They are rejected if the distance along the beam axis between the two vertices is larger than 0.8 cm, and if both vertices have at least three associated tracklets. This removes 48% of the pile-up events. In the remaining cases two events can be merged into a single one, thus yielding a biased multiplicity estimation. A simulation assuming a Gaussian distribution for the vertex z position results in a probability for the occurrence of two vertices closer than 0.8 cm of 7%. Combined with the pile-up rate of 4%, this gives an overall probability that two piled-up events are merged into a single event of $\approx 0.3\%$, which is a negligible contribution in the multiplicity ranges considered here.

The charged particle density $dN_{\text{ch}}/d\eta$ is calculated using the number of tracklets N_{trk} reconstructed from hits in the SPD detector, because the SPD is the only central barrel detector that is read out for all of the μ -MB trigger. The tracklets are required to point to the reconstructed interaction vertex within ± 1 cm in radial and ± 3 cm in z direction [31,32]. Using simulated events, it is verified that N_{trk} is proportional to $dN_{\text{ch}}/d\eta$. For a good geometrical coverage, only tracklets within $|\eta| < 1$ from events with $|z_{\text{vtx}}| < 10$ cm are considered. Since the pseudorapidity coverage of the SPD changes with the interaction vertex z position and also with time, due to the varying number of dead channels, a correction to the measured N_{trk} is applied event-by-event. This correction $C_{\text{trk}}(z_{\text{vtx}})$ is determined from measured data as a function of z_{vtx} by calculating the ratio of the number of tracklets reconstructed for a given z_{vtx} , $N_{\text{trk}}(z_{\text{vtx}})$, to the N_{trk} value measured for the z_{vtx} position with the maximal acceptance: $C_{\text{trk}}(z_{\text{vtx}}) = N_{\text{trk}}^{\text{max}}/N_{\text{trk}}(z_{\text{vtx}})$. It is found to be smaller than 10% for $|z_{\text{vtx}}| < 5$ cm and smaller than 25% for $|z_{\text{vtx}}| < 10$ cm. Fig. 1 shows the resulting distribution of the relative charged particle density $(dN_{\text{ch}}/d\eta)/(dN_{\text{ch}}/d\eta)$, where $\langle dN_{\text{ch}}/d\eta \rangle = 6.01 \pm 0.01(\text{stat.})_{-0.12}^{+0.20}(\text{syst.})$ as measured for inelastic pp collisions with at least one charged particle in $|\eta| < 1$ [32]. The use of relative quantities was chosen in order to facilitate the comparison to other experiments and to theoretical models, as well as to minimize systematic uncertainties. The definition of the charged particle multiplicity intervals used in this analysis is given in Table 1, together with the corresponding mean values of $dN_{\text{ch}}/d\eta$. The present statistics allows one to cover charged particle densities up to four times the minimum bias value.

¹ In the ALICE reference frame the muon spectrometer is located at negative z positions and thus negative (pseudo-)rapidities. Since pp collisions are symmetric relative to $y = 0$, we have dropped the minus sign when rapidities are quoted.

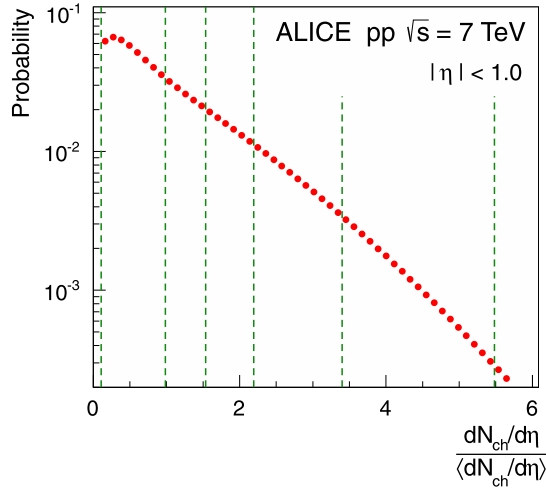


Fig. 1. The distribution of the relative charged particle density $(dN_{\text{ch}}/d\eta)/(dN_{\text{ch}}/d\eta)$ reconstructed around mid-rapidity ($|\eta| < 1.0$) after correction for SPD inefficiencies. The vertical lines indicate the boundaries of the multiplicity intervals used in this analysis.

For the J/ψ measurement in the di-electron channel tracks are selected by requiring a minimum p_t of 1 GeV/c, a pseudorapidity range of $|\eta| < 0.9$, at least 70 out of possible 159 points reconstructed in the TPC and an upper limit on the $\chi^2/\text{n.d.f.}$ from the momentum fit of 2.0. Furthermore, tracks that are not pointing back to the primary interaction vertex within 1.0 cm in the transverse plane and within 3.0 cm in z direction are discarded. To further reduce the background from conversion electrons a hit in at least one of the four innermost ITS layers is also required. Particle identification is performed by measuring the specific ionization dE/dx in the TPC. All tracks within $\pm 3\sigma$ around the expected dE/dx signal for electrons and at the same time outside $\pm 3\sigma$ ($\pm 3.5\sigma$) around the expectation for protons (pions) are accepted as electron and positron candidates. e^+ and e^- candidates that form a pair with any other candidate with an invariant mass below $0.1 \text{ GeV}/c^2$ are discarded to reduce the amount of electrons coming from γ conversions or π^0 Dalitz decays as well as their contribution to the combinatorial background in the di-electron invariant mass spectrum.

The invariant mass distributions of the e^+e^- pairs are recorded in intervals of the charged particle multiplicity as measured using the SPD tracklets. As an example, the lowest and highest multiplicity intervals are shown in the two left panels of Fig. 2. The combinatorial background in each multiplicity interval is well described by the track rotation method, which consists in rotating one of the tracks of a e^+e^- pair measured in a given event around the z axis by a random ϕ -angle in order to remove any correlations. After subtracting the background, the uncorrected J/ψ yields are obtained by integrating the distribution in the mass range $2.92\text{--}3.16 \text{ GeV}/c^2$. This range was chosen in order to maximize

the significance of the J/ψ signal. A fit to the invariant mass distribution for the sum of all multiplicity intervals after background subtraction with a Crystal Ball function [33] gives a mass resolution of $28.3 \pm 1.8 \text{ MeV}/c^2$. It was verified that the measured line shape is reproduced by the Monte Carlo simulation (see Fig. 2 in Ref. [8]). Alternatively, the combinatorial background is estimated by like-sign distributions, $N^{++} + N^{--}$. These are scaled to match the integral of the opposite-sign distributions in the mass range above the J/ψ signal ($3.2 < m_{\text{inv}} < 4.9 \text{ GeV}/c^2$) in order to also account for correlated background contributions, which mainly originates from semi-leptonic charm decays. Both methods provide a good description of the combinatorial background and their comparison is used to evaluate the systematic uncertainty on the J/ψ signal.

For the J/ψ analysis in the di-muon channel muon candidates are selected using the tracks measured in the tracking chambers behind the frontal absorber and requiring that at least one of the two tracks matches a trigger track reconstructed from at least three hits in the trigger chambers. This efficiently rejects hadrons produced in the frontal absorber and then absorbed by the iron wall positioned in front of the trigger chambers. Furthermore, a cut $R_{\text{abs}} > 17.5 \text{ cm}$ is applied, where R_{abs} is the radial coordinate of the track at the downstream end of the frontal absorber ($z = -5.03 \text{ m}$). Such a cut removes muons produced at small angles that have crossed a significant fraction of the conical absorber surrounding the beam pipe. Finally, a cut on the pair rapidity ($2.5 < y < 4$) is applied to reject events very close to the edge of the spectrometer acceptance.

The number of J/ψ in each multiplicity interval is obtained by fitting the corresponding di-muon invariant mass distribution in the range $2 < m_{\text{inv}} < 5 \text{ GeV}/c^2$. The line shapes of the J/ψ and $\psi(2S)$ are parametrized using Crystal Ball functions [33], while the underlying continuum is fitted with the sum of two exponential functions. The parameters of the Crystal Ball functions are adjusted to the mass distribution of a Monte Carlo signal sample, obtained by generating J/ψ and $\psi(2S)$ events with realistic phase space distributions [8]. Apart from the J/ψ and $\psi(2S)$ signal normalization, only the position of the J/ψ mass pole, as well as its width, are kept as free parameters in the fit. Due to the small statistics, the $\psi(2S)$ mass and width are tied to those of the J/ψ , imposing the mass difference between the two states to be equal to the one given by the Particle Data Group (PDG) [34], and the ratio of the resonance widths to be equal to the one obtained by analyzing reconstructed Monte Carlo events. Details on the fit technique can be found in [8]. The width of the J/ψ signal as obtained by fitting the Crystal Ball function to the invariant mass distribution for the sum of all multiplicity intervals is $\sigma_{J/\psi} = 83 \pm 3 \text{ MeV}/c^2$. The two right panels of Fig. 2 show the measured di-muon invariant mass distributions together with the results of the fit procedure for the lowest and highest multiplicity intervals.

The results are presented as the ratios of the J/ψ yield in a given multiplicity interval relative to the minimum bias yield. By performing simulation studies in intervals of $dN_{\text{ch}}/d\eta$ it was veri-

Table 1

The boundaries of the used charged particle multiplicity intervals as defined via the number of SPD tracklets N_{trk} , the corresponding charged particle density ranges and mean values $\langle dN_{\text{ch}}/d\eta(\text{bin}) \rangle$, as well as the number of analyzed minimum bias triggered events in the di-electron ($N_{\text{evt.}}^{e^+e^-}$) and the di-muon channel ($N_{\text{eq. evt.}}^{\mu^+\mu^-}$). In the latter case this is the equivalent number of events, derived from the number of μ -MB triggered events.

Multiplicity interval	N_{trk} interval	$dN_{\text{ch}}/d\eta$ range	$\langle dN_{\text{ch}}/d\eta(\text{bin}) \rangle$	$N_{\text{evt.}}^{e^+e^-} \times 10^6$	$N_{\text{eq. evt.}}^{\mu^+\mu^-} \times 10^6$
1	[1, 8]	0.7–5.9	2.7	164.6	262.0
2	[9, 13]	5.9–9.2	7.1	51.1	79.5
3	[14, 19]	9.2–13.2	10.7	35.7	55.4
4	[20, 30]	13.2–20.4	15.8	28.5	44.4
5	[31, 49]	20.4–32.9	24.1	9.7	15.3

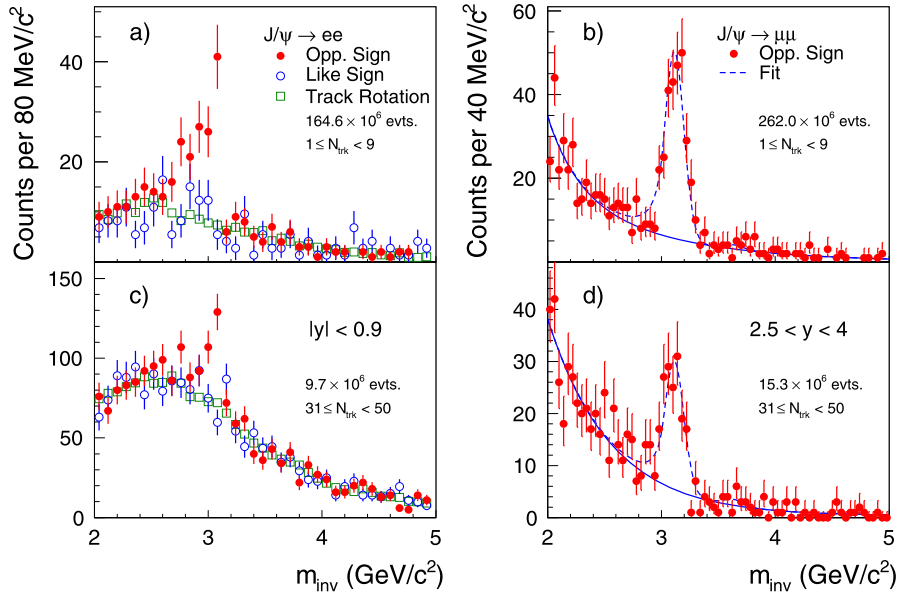


Fig. 2. Opposite sign invariant mass spectra of the selected electron [(a) + (c)] and muon [(b) + (d)] pairs (filled symbols) for the lowest [(a) + (b)] and highest [(c) + (d)] multiplicity intervals. Also shown are the estimates of the combinatorial background which are based on a fit to the $\mu^+\mu^-$ pair distributions (solid line), and on like-sign pairs (open circles), as well as track rotation (open squares), in the e^+e^- case. The number of events quoted in the figures refer to the corresponding minimum bias triggered events.

fied that the geometrical acceptances, as well as the reconstruction efficiencies and the J/ψ line shapes, do not depend on $dN_{ch}/d\eta$ in the range under consideration here ($dN_{ch}/d\eta < 32.9$). Therefore, these corrections and their corresponding systematic uncertainties cancel in the ratio $\langle dN_{J/\psi}/dy \rangle / \langle dN_{ch}/d\eta \rangle$ and only the uncorrected signal counts have to be divided. The number of events used for the normalization of $\langle dN_{J/\psi}/dy \rangle$ is corrected for the fraction of inelastic events not seen by the MB trigger condition. After applying acceptance and efficiency corrections these values are in agreement with those that can be obtained from the numbers quoted in [8]: $\langle dN_{J/\psi}/dy \rangle = (8.2 \pm 0.8(\text{stat.}) \pm 1.2(\text{syst.})) \times 10^{-5}$ for $J/\psi \rightarrow e^+e^-$ in $|y| < 0.9$, and $\langle dN_{J/\psi}/dy \rangle = (5.8 \pm 0.2(\text{stat.}) \pm 0.6(\text{syst.})) \times 10^{-5}$ for $J/\psi \rightarrow \mu^+\mu^-$ in $2.5 < y < 4$. In the case of the J/ψ yields measured in a given multiplicity interval, no trigger-related correction is needed, since the trigger efficiency is 100% for $N_{trk} \geq 1$.

The systematic uncertainties are estimated as follows. In case of the di-electron analysis, the absolute differences between the resulting $\langle dN_{J/\psi}/dy \rangle / \langle dN_{ch}/d\eta \rangle$ values obtained by using the like-sign and the track rotation methods define the uncertainty due to the background subtraction. It is found to vary between 2% and 12% for the different multiplicity intervals. For the di-muon analysis this uncertainty is evaluated by varying the functional form of the background description (polynomial instead of sum of two exponential). It depends on the signal to background ratio and varies between 3% and 4%. Since for the muon measurement it is not possible to associate a measured track to the interaction vertex, due to the multiple scattering of the muons in the frontal absorber, an additional systematic uncertainty arises from pile-up events. Among the vertices inside these events always the one with the largest number of associated tracks is chosen as main vertex. Therefore, events with very low multiplicities are more likely to have a wrong assignment and thus this uncertainty is largest in the first multiplicity interval (6%), while it is 3% in the others. Possible changes of the p_t spectra with event multiplicity can introduce a $dN_{ch}/d\eta$ dependence of the acceptance and efficiency correction, thus resulting in an additional systematic uncertainty. This is estimated by varying the $\langle p_t \rangle$ of the J/ψ spectrum that is used as input to the determination of the corrections via simulation between

2.6 and 3.2 GeV/c. A systematic effect of 1.5% (3.5%) is found for the di-electron (di-muon) analysis. The total systematic error on $\langle dN_{J/\psi}/dy \rangle / \langle dN_{ch}/d\eta \rangle$ is given by the quadratic sum of the separated contributions and amounts to 2.5–12% depending on the multiplicity interval for the di-electron result. In the case of the di-muon analysis it varies between 8% in the first and 6% in the last multiplicity interval. An additional global uncertainty of 1.5% on the normalization of $\langle dN_{J/\psi}/dy \rangle$ is introduced by the correction of the trigger inefficiency for all inelastic collisions.

The systematic uncertainties on $\langle dN_{ch}/d\eta \rangle / \langle dN_{ch}/d\eta \rangle$ are due to deviations from a linear dependence of $dN_{ch}/d\eta$ on N_{trk} and variations in the N_{trk} distributions which remain after the correction procedure. The latter are caused by changes in the SPD acceptance for the different data taking periods. The first contribution is estimated to be 5%, while the second is $\sim 2\%$, as determined by Monte Carlo studies. In addition, the systematic uncertainty of the $\langle dN_{ch}/d\eta \rangle$ measurement ($^{+3.3\%}_{-2.0\%}$) [32] is also included.

Fig. 3 shows the relative J/ψ yields measured at forward and at mid-rapidity as a function of the relative charged particle density around mid-rapidity. An approximately linear increase of the relative J/ψ yield $\langle dN_{J/\psi}/dy \rangle / \langle dN_{ch}/d\eta \rangle$ with $\langle dN_{ch}/d\eta \rangle / \langle dN_{ch}/d\eta \rangle$ is observed in both rapidity ranges. The enhancement relative to minimum bias J/ψ yield is a factor of approximately 5 at $2.5 < y < 4$ (8 at $|y| < 0.9$) for events with four times the minimum bias charged particle multiplicity density.

An interpretation of the observed correlation between the J/ψ yield and the charged particle multiplicity is that J/ψ production is always accompanied by a strong hadronic activity, thus biasing the $dN_{ch}/d\eta$ distributions to higher values. Since this correlation extends over the three units of rapidity between the mid-rapidity $dN_{ch}/d\eta$ and the forward rapidity J/ψ measurement, it would have far reaching consequences on any model trying to describe J/ψ production in pp collisions.

In order to illustrate that the observed behavior cannot be understood by a simple $2 \rightarrow 2$ hard partonic scattering scenario, a prediction by PYTHIA 6.4.25 in the Perugia 2011 tune [35,36] is shown in Fig. 4 as an example. Only J/ψ directly produced in hard scatterings via the NRQCD framework [37] (MSEL = 63) are considered, whereas J/ψ resulting from the cluster formation processes

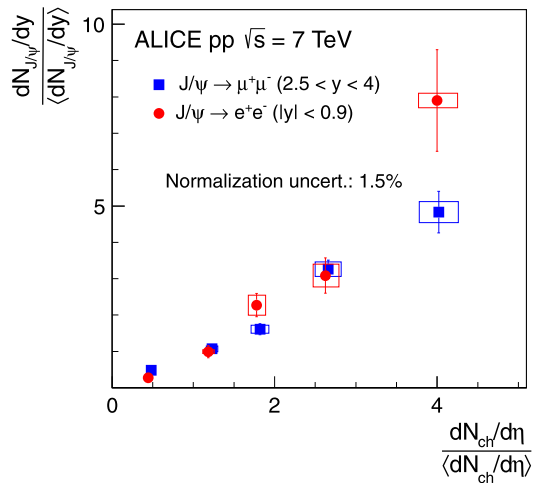


Fig. 3. J/ψ yield $dN_{J/\psi}/dy$ as a function of the charged particle multiplicity densities at mid-rapidity $dN_{ch}/d\eta$. Both values are normalized by the corresponding value for minimum bias pp collisions ($\langle dN_{J/\psi}/dy \rangle$, $\langle dN_{ch}/d\eta \rangle$). Shown are measurements at forward rapidities ($J/\psi \rightarrow \mu^+\mu^-$, $2.5 < y < 4$) and at mid-rapidity ($J/\psi \rightarrow e^+e^-$, $|y| < 0.9$). The error bars represent the statistical uncertainty on the J/ψ yields, while the quadratic sum of the point-by-point systematic uncertainties on the J/ψ yield as well as on $dN_{ch}/d\eta$ is depicted as boxes.

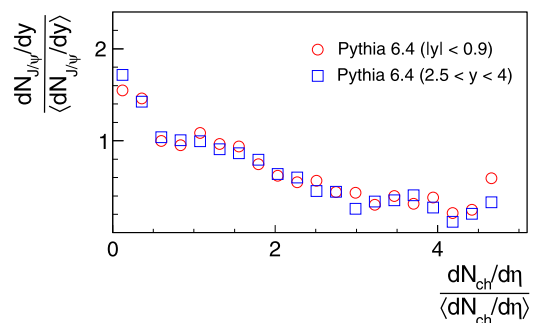


Fig. 4. Relative J/ψ yield $dN_{J/\psi}/dy$ as a function of relative charged particle multiplicity densities around mid-rapidity $dN_{ch}/d\eta$ as calculated with PYTHIA 6.4 in the Perugia 2011 tune [35,36]. Shown are results for directly produced J/ψ in hard scatterings via the NRQCD framework at forward rapidities ($2.5 < y < 4$) and at mid-rapidity ($|y| < 0.9$).

are ignored. A J/ψ cluster is a string formed by a $c\bar{c}$ pair produced via parton shower evolution which has an invariant mass that is too low for the standard Lund string fragmentation procedure and thus does not correspond to a well-defined hard scattering process. The calculation shown in Fig. 4 is thus the ratio of the multiplicity distributions generated for minimum bias events and events containing J/ψ from hard scatterings. It exhibits a decrease of the J/ψ multiplicity with respect to the event multiplicity, which indicates that hard J/ψ production, as modeled by PYTHIA 6.4.25, is not accompanied by an increase of the total hadronic activity. Further studies with other models such as PYTHIA 8 [38] and Cascade [39] are needed. It should be pointed out that our measurement also includes J/ψ from the decay of beauty hadrons, which is not part of the shown PYTHIA result. The fraction of J/ψ from feed down can change with the event multiplicity and can therefore contribute to the observed multiplicity dependence. However, since this contribution is on the order of 10% [6,7,11] it might be only a small contribution to the observed differences between model and data.

On the other hand, the increase of the J/ψ production with event multiplicity, as reported here, might be due to MPI. In this scenario the multiplicity of charged particles is a direct measure-

ment of the number of partonic interactions in the pp events. If the effect of MPI extends into the regime of hard processes, also the J/ψ yield should scale with the number of partonic collisions and the observed correlation will result. It has even been conjectured in [40] that the increase of the J/ψ yield with $dN_{ch}/d\eta$ and the ridge phenomenon observed in high-multiplicity pp collisions [23] could be related. They might both be caused by the lateral extent of the gluon distributions, in combination with fluctuations of the gluon density. The presence of these fluctuations could significantly increase the probability for MPI and thus cause the observed rise of the J/ψ yield.

The multiplicity dependence measured here will allow a direct comparison of the J/ψ production in pp to the one observed in heavy-ion collisions. With a mean value of $dN_{ch}/d\eta$ of 24.1, the highest multiplicity interval shown in Fig. 3, for instance, corresponds roughly to 45–50% centrality for Cu–Cu collisions at $\sqrt{s_{NN}} = 200$ GeV [21]. In order to establish whether any evidence for a J/ψ suppression is observed already in pp, a proper normalization is needed. This could be provided by a measurement of open charm production in the same multiplicity bins. Corresponding studies are currently ongoing.

In summary, relative J/ψ yields are measured for the first time in pp collisions as a function of the charged particle multiplicity density $dN_{ch}/d\eta$. J/ψ mesons are detected at mid-rapidity ($|y| < 0.9$) and forward rapidity ($2.5 < y < 4$), while $dN_{ch}/d\eta$ is determined at mid-rapidity ($|y| < 1$). An approximately linear increase of the J/ψ yields with the charged particle multiplicity is observed. The increase is similar at forward and mid-rapidity, exhibiting an enhancement relative to minimum bias J/ψ yield by a factor of about 5 at $2.5 < y < 4$ (8 at $|y| < 0.9$) for events with four times the minimum bias charged particle multiplicity. Our result might either indicate that J/ψ production in pp collisions is always connected with a strong hadronic activity, or that multiparton interactions could also affect the harder momentum scales relevant for quarkonia production. Further studies of charged particle multiplicity dependence of J/ψ , Υ , and open charm production, also as a function of p_t , will shed more light on the nature of the observed effect.

Acknowledgements

The ALICE Collaboration would like to thank all its engineers and technicians for their invaluable contributions to the construction of the experiment and the CERN accelerator teams for the outstanding performance of the LHC complex.

The ALICE Collaboration acknowledges the following funding agencies for their support in building and running the ALICE detector:

Calouste Gulbenkian Foundation from Lisbon and Swiss Fonds Kidagan, Armenia;

Conselho Nacional de Desenvolvimento Científico e Tecnológico (CNPq), Financiadora de Estudos e Projetos (FINEP), Fundação de Amparo à Pesquisa do Estado de São Paulo (FAPESP);

National Natural Science Foundation of China (NSFC), the Chinese Ministry of Education (CMOE) and the Ministry of Science and Technology of China (MSTC);

Ministry of Education and Youth of the Czech Republic;

Danish Natural Science Research Council, the Carlsberg Foundation and the Danish National Research Foundation;

The European Research Council under the European Community's Seventh Framework Programme;

Helsinki Institute of Physics and the Academy of Finland;

French CNRS-IN2P3, the 'Region Pays de Loire', 'Region Alsace', 'Region Auvergne' and CEA, France;

German BMBF and the Helmholtz Association;

General Secretariat for Research and Technology, Ministry of Development, Greece;

Hungarian OTKA and National Office for Research and Technology (NKTH);

Department of Atomic Energy and Department of Science and Technology of the Government of India;

Istituto Nazionale di Fisica Nucleare (INFN) of Italy;

MEXT Grant-in-Aid for Specially Promoted Research, Japan;

Joint Institute for Nuclear Research, Dubna;

National Research Foundation of Korea (NRF);

CONACYT, DGAPA, México, ALFA-EC and the HELEN Program (High-Energy Physics Latin-American-European Network);

Stichting voor Fundamenteel Onderzoek der Materie (FOM) and the Nederlandse Organisatie voor Wetenschappelijk Onderzoek (NWO), Netherlands;

Research Council of Norway (NFR);

Polish Ministry of Science and Higher Education;

National Authority for Scientific Research – NASR (Autoritatea Națională pentru Cercetare Științifică – ANCS);

Federal Agency of Science of the Ministry of Education and Science of Russian Federation, International Science and Technology Center, Russian Academy of Sciences, Russian Federal Agency of Atomic Energy, Russian Federal Agency for Science and Innovations and CERN-INTAS;

Ministry of Education of Slovakia;

Department of Science and Technology, South Africa;

CIEMAT, EELA, Ministerio de Educación y Ciencia of Spain, Xunta de Galicia (Consellería de Educación), CEADEN, Cubaenergía, Cuba, and IAEA (International Atomic Energy Agency);

Swedish Research Council (VR) and Knut & Alice Wallenberg Foundation (KAW);

Ukraine Ministry of Education and Science;

United Kingdom Science and Technology Facilities Council (STFC);

The United States Department of Energy, the United States National Science Foundation, the State of Texas, and the State of Ohio.

Open access

This article is published Open Access at sciencedirect.com. It is distributed under the terms of the Creative Commons Attribution License 3.0, which permits unrestricted use, distribution, and

reproduction in any medium, provided the original authors and source are credited.

References

- [1] N. Brambilla, et al., *Eur. Phys. J. C* 71 (2011) 1534.
- [2] J.P. Lansberg, *Eur. Phys. J. C* 61 (2009) 693.
- [3] Y. Ma, K. Wang, K. Chao, *Phys. Rev. Lett.* 106 (2011) 042002.
- [4] M. Butenschoen, B.A. Kniehl, *Phys. Rev. Lett.* 106 (2011) 022003.
- [5] M. Butenschoen, B.A. Kniehl, arXiv:1201.1872.
- [6] G. Aad, et al., ATLAS Collaboration, *Nucl. Phys. B* 850 (2011) 387.
- [7] R. Aaij, et al., LHCb Collaboration, *Eur. Phys. J. C* 71 (2011) 1645.
- [8] K. Aamodt, et al., ALICE Collaboration, *Phys. Lett. B* 704 (2011) 442.
- [9] B. Abelev, et al., ALICE Collaboration, *Phys. Rev. Lett.* 108 (2012) 082001.
- [10] V. Khachatryan, et al., CMS Collaboration, *Eur. Phys. J. C* 71 (2011) 1575.
- [11] S. Chatrchyan, et al., CMS Collaboration, *JHEP* 1202 (2012) 011.
- [12] T. Sjöstrand, M. van Zijl, *Phys. Rev. D* 36 (1987) 2019.
- [13] P. Bartalini, et al., arXiv:1003.4220.
- [14] D. Acosta, et al., CDF Collaboration, *Phys. Rev. D* 70 (2004) 072002.
- [15] V. Khachatryan, et al., CMS Collaboration, *Eur. Phys. J. C* 70 (2010) 555.
- [16] G. Aad, et al., ATLAS Collaboration, arXiv:1012.0791.
- [17] S. Porteboeuf, R. Granier de Cassagnac, *Nucl. Phys. B (Proc. Suppl.)* 214 (2011) 181.
- [18] M. Aguilar-Benitez, et al., NA27 Collaboration, *Z. Phys. C* 41 (1988) 191.
- [19] L. Frankfurt, M. Strikman, D. Treleani, C. Weiss, *Phys. Rev. Lett.* 101 (2008) 202003.
- [20] M. Strikman, *Prog. Theor. Phys. Suppl.* 187 (2011) 289.
- [21] B. Alver, et al., PHOBOS Collaboration, *Phys. Rev. C* 83 (2011) 024913.
- [22] W. Li, et al., CMS Collaboration, *J. Phys. G* 38 (2011) 124027.
- [23] V. Khachatryan, et al., CMS Collaboration, *JHEP* 1009 (2010) 091.
- [24] T. Matsui, H. Satz, *Phys. Lett. B* 178 (1986) 416.
- [25] A. Andronic, P. Braun-Munzinger, K. Redlich, J. Stachel, *Phys. Lett. B* 571 (2003) 36.
- [26] C. Miao, A. Mocsy, P. Petreczky, *Nucl. Phys. A* 855 (2011) 125.
- [27] K. Aamodt, et al., ALICE Collaboration, *JINST* 3 (2008) S08002.
- [28] K. Aamodt, et al., ALICE Collaboration, *JINST* 5 (2010) P03003.
- [29] J. Alme, et al., *Nucl. Instrum. Meth. A* 622 (2010) 316.
- [30] K. Aamodt, et al., ALICE Collaboration, Measurement of inelastic, single and double diffraction cross sections in proton–proton collisions at LHC with ALICE, in preparation.
- [31] K. Aamodt, et al., ALICE Collaboration, *Eur. Phys. J. C* 68 (2010) 89.
- [32] K. Aamodt, et al., ALICE Collaboration, *Eur. Phys. J. C* 68 (2010) 345.
- [33] J.E. Gaiser, PhD thesis, SLAC-R-255, 1982.
- [34] K. Nakamura, et al., Particle Data Group, *J. Phys. G* 37 (2010) 075021.
- [35] P.Z. Skands, *Phys. Rev. D* 82 (2010) 074018.
- [36] T. Sjöstrand, S. Mrenna, P.Z. Skands, *JHEP* 0605 (2006) 026.
- [37] G.T. Bodwin, E. Braaten, G.P. Lepage, *Phys. Rev. D* 51 (1995) 1125.
- [38] T. Sjöstrand, S. Mrenna, P.Z. Skands, *Comput. Phys. Commun.* 178 (2008) 852.
- [39] H. Jung, *Comput. Phys. Commun.* 143 (2002) 100.
- [40] M. Strikman, *Phys. Rev. D* 84 (2011) 011501(R).

ALICE Collaboration

B. Abelev⁶⁸, J. Adam³³, D. Adamová⁷³, A.M. Adare¹²⁰, M.M. Aggarwal⁷⁷, G. Aglieri Rinella²⁹, A.G. Agocs⁶⁰, A. Agostinelli²¹, S. Aguilar Salazar⁵⁶, Z. Ahammed¹¹⁶, A. Ahmad Masoodi¹³, N. Ahmad¹³, S.U. Ahn^{63,36}, A. Akindinov⁴⁶, D. Aleksandrov⁸⁸, B. Alessandro⁹⁴, R. Alfaro Molina⁵⁶, A. Alici^{97,9}, A. Alkin², E. Almaráz Aviña⁵⁶, J. Alme³¹, T. Alt³⁵, V. Altini²⁷, S. Altinpinar¹⁴, I. Altsybeev¹¹⁷, C. Andrei⁷⁰, A. Andronic⁸⁵, V. Anguelov⁸², J. Anielski⁵⁴, C. Anson¹⁵, T. Antičić⁸⁶, F. Antinori⁹³, P. Antonioli⁹⁷, L. Aphecetche¹⁰², H. Appelshäuser⁵², N. Arbor⁶⁴, S. Arcelli²¹, A. Arend⁵², N. Armesto¹², R. Arnaldi⁹⁴, T. Aronsson¹²⁰, I.C. Arsene⁸⁵, M. Arslanok⁵², A. Asryan¹¹⁷, A. Augustinus²⁹, R. Auerbach⁸⁵, T.C. Awes⁷⁴, J. Äystö³⁷, M.D. Azmi¹³, M. Bach³⁵, A. Badalà⁹⁹, Y.W. Baek^{63,36}, R. Bailhache⁵², R. Bala⁹⁴, R. Baldini Ferrolì⁹, A. Baldisseri¹¹, A. Baldit⁶³, F. Baltasar Dos Santos Pedrosa²⁹, J. Bán⁴⁷, R.C. Baral⁴⁸, R. Barbera²³, F. Barile²⁷, G.G. Barnaföldi⁶⁰, L.S. Barnby⁹⁰, V. Barret⁶³, J. Bartke¹⁰⁴, M. Basile²¹, N. Bastid⁶³, B. Bathen⁵⁴, G. Batigne¹⁰², B. Batyunya⁵⁹, C. Baumann⁵², I.G. Bearden⁷¹, H. Beck⁵², I. Belikov⁵⁸, F. Bellini²¹, R. Bellwied¹¹⁰, E. Belmont-Moreno⁵⁶, G. Bencedi⁶⁰, S. Beole²⁵, I. Berceau⁷⁰, A. Bercuci⁷⁰, Y. Berdnikov⁷⁵, D. Berenyi⁶⁰, C. Bergmann⁵⁴, D. Berzano⁹⁴, L. Betev²⁹, A. Bhasin⁸⁰, A.K. Bhati⁷⁷, N. Bianchi⁶⁵, L. Bianchi²⁵, C. Bianchin¹⁹, J. Bielčík³³, J. Bielčíková⁷³, A. Bilandzic⁷², S. Bjelogrić⁴⁵, F. Blanco¹¹⁰,

F. Blanco⁷, D. Blau⁸⁸, C. Blume^{52,*}, M. Boccioni²⁹, N. Bock¹⁵, A. Bogdanov⁶⁹, H. Bøggild⁷¹, M. Bogolyubsky⁴³, L. Boldizsár⁶⁰, M. Bombara³⁴, J. Book⁵², H. Borel¹¹, A. Borisov¹¹⁹, S. Bose⁸⁹, F. Bossú²⁵, M. Botje⁷², S. Böttger⁵¹, B. Boyer⁴², P. Braun-Munzinger⁸⁵, M. Bregant¹⁰², T. Breitner⁵¹, T.A. Browning⁸³, M. Broz³², R. Brun²⁹, E. Bruna^{25,94}, G.E. Bruno²⁷, D. Budnikov⁸⁷, H. Buesching⁵², S. Bufalino^{25,94}, K. Bugaiev², O. Busch⁸², Z. Buthelezi⁷⁹, D. Caballero Orduna¹²⁰, D. Caffarri¹⁹, X. Cai³⁹, H. Caines¹²⁰, E. Calvo Villar⁹¹, P. Camerini²⁰, V. Canoa Roman^{8,1}, G. Cara Romeo⁹⁷, F. Carena²⁹, W. Carena²⁹, N. Carlin Filho¹⁰⁷, F. Carminati²⁹, C.A. Carrillo Montoya²⁹, A. Casanova Díaz⁶⁵, J. Castillo Castellanos¹¹, J.F. Castillo Hernandez⁸⁵, E.A.R. Casula¹⁸, V. Catanescu⁷⁰, C. Cavicchioli²⁹, J. Cepila³³, P. Cerello⁹⁴, B. Chang^{37,123}, S. Chapeland²⁹, J.L. Charvet¹¹, S. Chattopadhyay⁸⁹, S. Chattopadhyay¹¹⁶, M. Cherney⁷⁶, C. Cheshkov^{29,109}, B. Cheynis¹⁰⁹, E. Chiavassa⁹⁴, V. Chibante Barroso²⁹, D.D. Chinellato¹⁰⁸, P. Chochula²⁹, M. Chojnacki⁴⁵, P. Christakoglou^{72,45}, C.H. Christensen⁷¹, P. Christiansen²⁸, T. Chujo¹¹⁴, S.U. Chung⁸⁴, C. Cicalo⁹⁶, L. Cifarelli^{21,29}, F. Cindolo⁹⁷, J. Cleymans⁷⁹, F. Coccetti⁹, F. Colamaria²⁷, D. Colella²⁷, G. Conesa Balbastre⁶⁴, Z. Conesa del Valle²⁹, P. Constantin⁸², G. Contin²⁰, J.G. Contreras⁸, T.M. Cormier¹¹⁹, Y. Corrales Morales²⁵, P. Cortese²⁶, I. Cortés Maldonado¹, M.R. Cosentino^{67,108}, F. Costa²⁹, M.E. Cotallo⁷, E. Crescio⁸, P. Crochet⁶³, E. Cruz Alaniz⁵⁶, E. Cuautle⁵⁵, L. Cunqueiro⁶⁵, A. Dainese^{19,93}, H.H. Dalsgaard⁷¹, A. Danu⁵⁰, I. Das^{89,42}, K. Das⁸⁹, D. Das⁸⁹, S. Dash^{40,94}, A. Dash¹⁰⁸, S. De¹¹⁶, A. De Azevedo Moregula⁶⁵, G.O.V. de Barros¹⁰⁷, A. De Caro^{24,9}, G. de Cataldo⁹⁸, J. de Cuveland³⁵, A. De Falco¹⁸, D. De Gruttola²⁴, H. Delagrange¹⁰², E. Del Castillo Sanchez²⁹, A. Deloff¹⁰⁰, V. Demanov⁸⁷, N. De Marco⁹⁴, E. Dénes⁶⁰, S. De Pasquale²⁴, A. Deppman¹⁰⁷, G.D. Erasmo²⁷, R. de Rooij⁴⁵, D. Di Bari²⁷, T. Dietel⁵⁴, C. Di Giglio²⁷, S. Di Liberto⁹⁵, A. Di Mauro²⁹, P. Di Nezza⁶⁵, R. Divià²⁹, Ø. Djuvsland¹⁴, A. Dobrin^{119,28}, T. Dobrowolski¹⁰⁰, I. Domínguez⁵⁵, B. Dönigus⁸⁵, O. Dordic¹⁷, O. Driga¹⁰², A.K. Dubey¹¹⁶, L. Ducroux¹⁰⁹, P. Dupieux⁶³, A.K. Dutta Majumdar⁸⁹, M.R. Dutta Majumdar¹¹⁶, D. Elia⁹⁸, D. Emschermann⁵⁴, H. Engel⁵¹, H.A. Erdal³¹, B. Espagnon⁴², M. Estienne¹⁰², S. Esumi¹¹⁴, D. Evans⁹⁰, G. Eyyubova¹⁷, D. Fabris^{19,93}, J. Faivre⁶⁴, D. Falchieri²¹, A. Fantoni⁶⁵, M. Fasel⁸⁵, R. Fearick⁷⁹, A. Fedunov⁵⁹, D. Fehlinger¹⁴, L. Feldkamp⁵⁴, D. Felea⁵⁰, G. Feofilov¹¹⁷, A. Fernández Téllez¹, R. Ferretti²⁶, A. Ferretti²⁵, J. Figiel¹⁰⁴, M.A.S. Figueredo¹⁰⁷, S. Filchagin⁸⁷, D. Finogeev⁴⁴, F.M. Fionda²⁷, E.M. Fiore²⁷, M. Floris²⁹, S. Foertsch⁷⁹, P. Foka⁸⁵, S. Fokin⁸⁸, E. Fragiaco⁹², M. Fragkiadakis⁷⁸, U. Frankenfild⁸⁵, U. Fuchs²⁹, C. Furget⁶⁴, M. Fusco Girard²⁴, J.J. Gaardhøje⁷¹, M. Gagliardi²⁵, A. Gago⁹¹, M. Gallio²⁵, D.R. Gangadharan¹⁵, P. Ganoti⁷⁴, C. Garabatos⁸⁵, E. Garcia-Solis¹⁰, I. Garishvili⁶⁸, J. Gerhard³⁵, M. Germain¹⁰², C. Geuna¹¹, A. Gheata²⁹, M. Gheata²⁹, B. Ghidini²⁷, P. Ghosh¹¹⁶, P. Gianotti⁶⁵, M.R. Girard¹¹⁸, P. Giubellino²⁹, E. Gladysz-Dziadus¹⁰⁴, P. Glässel⁸², R. Gomez¹⁰⁶, E.G. Ferreira¹², L.H. González-Trueba⁵⁶, P. González-Zamora⁷, S. Gorbunov³⁵, A. Goswami⁸¹, S. Gotovac¹⁰³, V. Grabski⁵⁶, L.K. Graczykowski¹¹⁸, R. Grajcarek⁸², A. Grelli⁴⁵, A. Grigoras²⁹, C. Grigoras²⁹, V. Grigoriev⁶⁹, A. Grigoryan¹²¹, S. Grigoryan⁵⁹, B. Grinyov², N. Grion⁹², P. Gros²⁸, J.F. Grosse-Oetringhaus²⁹, J.-Y. Grossiord¹⁰⁹, R. Grosso²⁹, F. Guber⁴⁴, R. Guernane⁶⁴, C. Guerra Gutierrez⁹¹, B. Guerzoni²¹, M. Guilbaud¹⁰⁹, K. Gulbrandsen⁷¹, T. Gunji¹¹³, A. Gupta⁸⁰, R. Gupta⁸⁰, H. Gutbrod⁸⁵, Ø. Haaland¹⁴, C. Hadjidakis⁴², M. Haiduc⁵⁰, H. Hamagaki¹¹³, G. Hamar⁶⁰, B.H. Han¹⁶, L.D. Hanratty⁹⁰, A. Hansen⁷¹, Z. Harmanova³⁴, J.W. Harris¹²⁰, M. Hartig⁵², D. Hasegan⁵⁰, D. Hatzifotiadou⁹⁷, A. Hayrapetyan^{29,121}, S.T. Heckel⁵², M. Heide⁵⁴, H. Helstrup³¹, A. Herghelegiu⁷⁰, G. Herrera Corral⁸, N. Herrmann⁸², K.F. Hetland³¹, B. Hicks¹²⁰, P.T. Hille¹²⁰, B. Hippolyte⁵⁸, T. Horaguchi¹¹⁴, Y. Hori¹¹³, P. Hristov²⁹, I. Hřivnáčová⁴², M. Huang¹⁴, S. Huber⁸⁵, T.J. Humanic¹⁵, D.S. Hwang¹⁶, R. Ichou⁶³, R. Ilkaev⁸⁷, I. Ilkiv¹⁰⁰, M. Inaba¹¹⁴, E. Incani¹⁸, G.M. Innocenti²⁵, P.G. Innocenti²⁹, M. Ippolitov⁸⁸, M. Irfan¹³, C. Ivan⁸⁵, M. Ivanov⁸⁵, A. Ivanov¹¹⁷, V. Ivanov⁷⁵, O. Ivanytskyi², A. Jachołkowski²⁹, P.M. Jacobs⁶⁷, L. Jancurová⁵⁹, H.J. Jang⁶², S. Jangal⁵⁸, M.A. Janik¹¹⁸, R. Janik³², P.H.S.Y. Jayarathna¹¹⁰, S. Jena⁴⁰, R.T. Jimenez Bustamante⁵⁵, L. Jirden²⁹, P.G. Jones⁹⁰, H. Jung³⁶, W. Jung³⁶, A. Jusko⁹⁰, A.B. Kaidalov⁴⁶, V. Kakoyan¹²¹, S. Kalcher³⁵, P. Kaliňák⁴⁷, M. Kalisky⁵⁴, T. Kalliokoski³⁷, A. Kalweit⁵³, K. Kanaki¹⁴, J.H. Kang¹²³, V. Kaplin⁶⁹, A. Karasu Uysal^{29,122}, O. Karavichev⁴⁴, T. Karavicheva⁴⁴, E. Karpechev⁴⁴, A. Kazantsev⁸⁸, U. Keschull⁵¹, R. Keidel¹²⁴, S.A. Khan¹¹⁶, M.M. Khan¹³, P. Khan⁸⁹, A. Khanzadeev⁷⁵, Y. Kharlov⁴³, B. Kileng³¹, M. Kim¹²³, T. Kim¹²³, S. Kim¹⁶, D.J. Kim³⁷, J.H. Kim¹⁶, J.S. Kim³⁶, S.H. Kim³⁶, D.W. Kim³⁶, B. Kim¹²³, S. Kirsch^{35,29}, I. Kisel³⁵, S. Kiselev⁴⁶, A. Kisiel^{29,118}, J.L. Klay⁴, J. Klein⁸², C. Klein-Bösing⁵⁴,

M. Kliemant⁵², A. Kluge²⁹, M.L. Knichel⁸⁵, A.G. Knospe¹⁰⁵, K. Koch⁸², M.K. Köhler⁸⁵, A. Kolojvari¹¹⁷,
 V. Kondratiev¹¹⁷, N. Kondratyeva⁶⁹, A. Konevskikh⁴⁴, A. Korneev⁸⁷, C. Kottachchi Kankanamge Don¹¹⁹,
 R. Kour⁹⁰, M. Kowalski¹⁰⁴, S. Kox⁶⁴, G. Koyithatta Meethalevedu⁴⁰, J. Kral³⁷, I. Králik⁴⁷, F. Kramer⁵²,
 I. Kraus⁸⁵, T. Krawutschke^{82,30}, M. Krelina³³, M. Kretz³⁵, M. Krivda^{90,47}, F. Krizek³⁷, M. Krus³³,
 E. Kryshen⁷⁵, M. Krzewicki^{72,85}, Y. Kucheriaev⁸⁸, C. Kuhn⁵⁸, P.G. Kuijjer⁷², P. Kurashvili¹⁰⁰,
 A.B. Kurepin⁴⁴, A. Kurepin⁴⁴, A. Kuryakin⁸⁷, V. Kushpil⁷³, S. Kushpil⁷³, H. Kvaerno¹⁷, M.J. Kweon⁸²,
 Y. Kwon¹²³, P. Ladrón de Guevara⁵⁵, I. Lakomov^{42,117}, R. Langoy¹⁴, C. Lara⁵¹, A. Lardeux¹⁰²,
 P. La Rocca²³, C. Lazzeroni⁹⁰, R. Lea²⁰, Y. Le Bornec⁴², K.S. Lee³⁶, S.C. Lee³⁶, F. Lefèvre¹⁰², J. Lehnert⁵²,
 L. Leistam²⁹, M. Lenhardt¹⁰², V. Lenti⁹⁸, H. León⁵⁶, I. León Monzón¹⁰⁶, H. León Vargas⁵², P. Lévai⁶⁰,
 J. Lien¹⁴, R. Lietava⁹⁰, S. Lindal¹⁷, V. Lindenstruth³⁵, C. Lippmann^{85,29}, M.A. Lisa¹⁵, L. Liu¹⁴,
 P.I. Loenne¹⁴, V.R. Loggins¹¹⁹, V. Loginov⁶⁹, S. Lohn²⁹, D. Lohner⁸², C. Loizides⁶⁷, K.K. Loo³⁷,
 X. Lopez⁶³, E. López Torres⁶, G. Løvholden¹⁷, X.-G. Lu⁸², P. Luettig⁵², M. Lunardon¹⁹, J. Luo³⁹,
 G. Luparello⁴⁵, L. Luquin¹⁰², C. Luzzi²⁹, K. Ma³⁹, R. Ma¹²⁰, D.M. Madagodahettige-Don¹¹⁰,
 A. Maevskaya⁴⁴, M. Mager^{53,29}, D.P. Mahapatra⁴⁸, A. Maire⁵⁸, M. Malaev⁷⁵, I. Maldonado Cervantes⁵⁵,
 L. Malinina^{59,i}, D. Mal'Kevich⁴⁶, P. Malzacher⁸⁵, A. Mamonov⁸⁷, L. Manceau⁹⁴, L. Mangotra⁸⁰,
 V. Manko⁸⁸, F. Manso⁶³, V. Manzari⁹⁸, Y. Mao^{64,39}, M. Marchisone^{63,25}, J. Mareš⁴⁹,
 G.V. Margagliotti^{20,92}, A. Margotti⁹⁷, A. Marín⁸⁵, C.A. Marin Tobon²⁹, C. Markert¹⁰⁵, I. Martashvili¹¹²,
 P. Martinengo²⁹, M.I. Martínez¹, A. Martínez Davalos⁵⁶, G. Martínez García¹⁰², Y. Martynov²,
 A. Mas¹⁰², S. Masciocchi⁸⁵, M. Maserà²⁵, A. Masoni⁹⁶, L. Massacrier^{109,102}, M. Mastromarco⁹⁸,
 A. Mastroserio^{27,29}, Z.L. Matthews⁹⁰, A. Matyja^{104,102}, D. Mayani⁵⁵, C. Mayer¹⁰⁴, J. Mazer¹¹²,
 M.A. Mazzoni⁹⁵, F. Meddi²², A. Menchaca-Rocha⁵⁶, J. Mercado Pérez⁸², M. Meres³², Y. Miake¹¹⁴,
 L. Milano²⁵, J. Milosevic^{17,ii}, A. Mischke⁴⁵, A.N. Mishra⁸¹, D. Miśkowiec^{85,29}, C. Mitu⁵⁰, J. Mlynarz¹¹⁹,
 B. Mohanty¹¹⁶, A.K. Mohanty²⁹, L. Molnar²⁹, L. Montaña Zetina⁸, M. Monteno⁹⁴, E. Montes⁷,
 T. Moon¹²³, M. Morando¹⁹, D.A. Moreira De Godoy¹⁰⁷, S. Moretto¹⁹, A. Morsch²⁹, V. Muccifora⁶⁵,
 E. Mudnic¹⁰³, S. Muhuri¹¹⁶, H. Müller²⁹, M.G. Munhoz¹⁰⁷, L. Musa²⁹, A. Musso⁹⁴, B.K. Nandi⁴⁰,
 R. Nania⁹⁷, E. Nappi⁹⁸, C. Nattrass¹¹², N.P. Naumov⁸⁷, S. Navin⁹⁰, T.K. Nayak¹¹⁶, S. Nazarenko⁸⁷,
 G. Nazarov⁸⁷, A. Nedosekin⁴⁶, M. Nicassio²⁷, B.S. Nielsen⁷¹, T. Niida¹¹⁴, S. Nikolaev⁸⁸, V. Nikolic⁸⁶,
 S. Nikulin⁸⁸, V. Nikulin⁷⁵, B.S. Nilsen⁷⁶, M.S. Nilsson¹⁷, F. Noferini^{97,9}, P. Nomokonov⁵⁹, G. Nooren⁴⁵,
 N. Novitzky³⁷, A. Nyanin⁸⁸, A. Nyatha⁴⁰, C. Nygaard⁷¹, J. Nystrand¹⁴, A. Ochirov¹¹⁷, H. Oeschler^{53,29},
 S.K. Oh³⁶, S. Oh¹²⁰, J. Oleniacz¹¹⁸, C. Oppedisano⁹⁴, A. Ortiz Velasquez^{28,55}, G. Ortona²⁵,
 A. Oskarsson²⁸, P. Ostrowski¹¹⁸, J. Otwinowski⁸⁵, K. Oyama⁸², K. Ozawa¹¹³, Y. Pachmayer⁸²,
 M. Pachr³³, F. Padilla²⁵, P. Pagano²⁴, G. Paic⁵⁵, F. Painke³⁵, C. Pajares¹², S.K. Pal¹¹⁶, S. Pal¹¹,
 A. Palaha⁹⁰, A. Palmeri⁹⁹, V. Papikyan¹²¹, G.S. Pappalardo⁹⁹, W.J. Park⁸⁵, A. Passfeld⁵⁴,
 B. Pastirčák⁴⁷, D.I. Patalakha⁴³, V. Patricchio⁹⁸, A. Pavlinov¹¹⁹, T. Pawlak¹¹⁸, T. Peitzmann⁴⁵,
 E. Pereira De Oliveira Filho¹⁰⁷, D. Peresunko⁸⁸, C.E. Pérez Lara⁷², E. Perez Lezama⁵⁵, D. Perini²⁹,
 D. Perrino²⁷, W. Peryt¹¹⁸, A. Pesci⁹⁷, V. Peskov^{29,55}, Y. Pestov³, V. Petráček³³, M. Petran³³, M. Petris⁷⁰,
 P. Petrov⁹⁰, M. Petrovici⁷⁰, C. Petta²³, S. Piano⁹², A. Piccotti⁹⁴, M. Pikna³², P. Pillot¹⁰², O. Pinazza²⁹,
 L. Pinsky¹¹⁰, N. Pitz⁵², F. Piuz²⁹, D.B. Piyarathna¹¹⁰, M. Płoskoń⁶⁷, J. Pluta¹¹⁸, T. Pocheptsov^{59,17},
 S. Pochybova⁶⁰, P.L.M. Podesta-Lerma¹⁰⁶, M.G. Poghosyan^{29,25}, K. Polák⁴⁹, B. Polichtchouk⁴³, A. Pop⁷⁰,
 S. Porteboeuf-Houssais⁶³, V. Pospíšil³³, B. Potukuchi⁸⁰, S.K. Prasad¹¹⁹, R. Preghenella^{97,9}, F. Prino⁹⁴,
 C.A. Pruneau¹¹⁹, I. Pshenichnov⁴⁴, S. Puchagin⁸⁷, G. Puudu¹⁸, J. Pujol Teixido⁵¹, A. Pulvirenti^{23,29},
 V. Punin⁸⁷, M. Putiš³⁴, J. Putschke^{119,120}, E. Quercigh²⁹, H. Qvigstad¹⁷, A. Rachevski⁹²,
 A. Rademakers²⁹, S. Radomski⁸², T.S. Rähä³⁷, J. Rak³⁷, A. Rakotozafindrabe¹¹, L. Ramello²⁶,
 A. Ramírez Reyes⁸, S. Raniwala⁸¹, R. Raniwala⁸¹, S.S. Räsänen³⁷, B.T. Rascanu⁵², D. Rathee⁷⁷,
 K.F. Read¹¹², J.S. Real⁶⁴, K. Redlich^{100,57}, P. Reichelt⁵², M. Reicher⁴⁵, R. Renfordt⁵², A.R. Reolon⁶⁵,
 A. Reshetin⁴⁴, F. Rettig³⁵, J.-P. Revol²⁹, K. Reygers⁸², L. Riccati⁹⁴, R.A. Ricci⁶⁶, T. Richert²⁸, M. Richter¹⁷,
 P. Riedler²⁹, W. Riegler²⁹, F. Riggi^{23,99}, M. Rodríguez Cahuantzi¹, K. Røed¹⁴, D. Rohr³⁵, D. Röhrich¹⁴,
 R. Romita⁸⁵, F. Ronchetti⁶⁵, P. Rosnet⁶³, S. Rossegger²⁹, A. Rossi¹⁹, F. Roukoutakis⁷⁸, C. Roy⁵⁸, P. Roy⁸⁹,
 A.J. Rubio Montero⁷, R. Rui²⁰, E. Ryabinkin⁸⁸, A. Rybicki¹⁰⁴, S. Sadovsky⁴³, K. Šafařík²⁹, R. Sahoo⁴¹,
 P.K. Sahu⁴⁸, J. Saini¹¹⁶, H. Sakaguchi³⁸, S. Sakai⁶⁷, D. Sakata¹¹⁴, C.A. Salgado¹², J. Salzwedel¹⁵,
 S. Sambyal⁸⁰, V. Samsonov⁷⁵, X. Sanchez Castro^{55,58}, L. Šándor⁴⁷, A. Sandoval⁵⁶, S. Sano¹¹³,
 M. Sano¹¹⁴, R. Santo⁵⁴, R. Santoro^{98,29}, J. Sarkamo³⁷, E. Scapparone⁹⁷, F. Scarlassara¹⁹,

R.P. Scharenberg⁸³, C. Schiaua⁷⁰, R. Schicker⁸², C. Schmidt⁸⁵, H.R. Schmidt^{85,115}, S. Schreiner²⁹, S. Schuchmann⁵², J. Schukraft²⁹, Y. Schutz^{29,102}, K. Schwarz⁸⁵, K. Schweda^{85,82}, G. Scioli²¹, E. Scomparin⁹⁴, P.A. Scott⁹⁰, R. Scott¹¹², G. Segato¹⁹, I. Selyuzhenkov⁸⁵, S. Senyukov^{26,58}, J. Seo⁸⁴, S. Serici¹⁸, E. Serradilla^{7,56}, A. Sevcenco⁵⁰, I. Sgura⁹⁸, A. Shabetai¹⁰², G. Shabratova⁵⁹, R. Shahoyan²⁹, N. Sharma⁷⁷, S. Sharma⁸⁰, K. Shigaki³⁸, M. Shimomura¹¹⁴, K. Shtejer⁶, Y. Sibiriak⁸⁸, M. Siciliano²⁵, E. Sicking²⁹, S. Siddhanta⁹⁶, T. Siemiarczuk¹⁰⁰, D. Silvermyr⁷⁴, G. Simonetti^{27,29}, R. Singaraju¹¹⁶, R. Singh⁸⁰, S. Singha¹¹⁶, B.C. Sinha¹¹⁶, T. Sinha⁸⁹, B. Sitar³², M. Sitta²⁶, T.B. Skaali¹⁷, K. Skjerdal¹⁴, R. Smakal³³, N. Smirnov¹²⁰, R. Snellings⁴⁵, C. Søgaard⁷¹, R. Soltz⁶⁸, H. Son¹⁶, J. Song⁸⁴, M. Song¹²³, C. Soos²⁹, F. Soramel¹⁹, I. Sputowska¹⁰⁴, M. Spyropoulou-Stassinaki⁷⁸, B.K. Srivastava⁸³, J. Stachel⁸², I. Stan⁵⁰, I. Stan⁵⁰, G. Stefanek¹⁰⁰, G. Stefanini²⁹, T. Steinbeck³⁵, M. Steinpreis¹⁵, E. Stenlund²⁸, G. Steyn⁷⁹, D. Stocco¹⁰², M. Stolpovskiy⁴³, K. Strabykin⁸⁷, P. Strmen³², A.A.P. Suaide¹⁰⁷, M.A. Subieta Vásquez²⁵, T. Sugitate³⁸, C. Suire⁴², M. Sukhorukov⁸⁷, R. Sultanov⁴⁶, M. Šumbera⁷³, T. Susa⁸⁶, A. Szanto de Toledo¹⁰⁷, I. Szarka³², A. Szostak¹⁴, C. Tagridis⁷⁸, J. Takahashi¹⁰⁸, J.D. Tapia Takaki⁴², A. Tauro²⁹, G. Tejeda Muñoz¹, A. Telesca²⁹, C. Terrevoli²⁷, J. Thäder⁸⁵, D. Thomas⁴⁵, R. Tieulent¹⁰⁹, A.R. Timmins¹¹⁰, D. Tlusty³³, A. Toia^{35,29}, H. Torii^{38,113}, L. Toscano⁹⁴, F. Tosello⁹⁴, D. Truesdale¹⁵, W.H. Trzaska³⁷, T. Tsuji¹¹³, A. Tumkin⁸⁷, R. Turrisi⁹³, T.S. Tveter¹⁷, J. Ulery⁵², K. Ullaland¹⁴, J. Ulrich^{61,51}, A. Uras¹⁰⁹, J. Urbán³⁴, G.M. Urciuoli⁹⁵, G.L. Usai¹⁸, M. Vajzer^{33,73}, M. Vala^{59,47}, L. Valencia Palomo⁴², S. Vallero⁸², N. van der Kolk⁷², P. Vande Vyvre²⁹, M. van Leeuwen⁴⁵, L. Vannucci⁶⁶, A. Vargas¹, R. Varma⁴⁰, M. Vasileiou⁷⁸, A. Vasiliev⁸⁸, V. Vechernin¹¹⁷, M. Veldhoen⁴⁵, M. Venaruzzo²⁰, E. Vercellin²⁵, S. Vergara¹, D.C. Vernekohl⁵⁴, R. Vernet⁵, M. Verweij⁴⁵, L. Vickovic¹⁰³, G. Viesti¹⁹, O. Vikhlyantsev⁸⁷, Z. Vilakazi⁷⁹, O. Villalobos Baillie⁹⁰, A. Vinogradov⁸⁸, L. Vinogradov¹¹⁷, Y. Vinogradov⁸⁷, T. Virgili²⁴, Y.P. Viyogi¹¹⁶, A. Vodopyanov⁵⁹, K. Voloshin⁴⁶, S. Voloshin¹¹⁹, G. Volpe^{27,29}, B. von Haller²⁹, D. Vranic⁸⁵, G. Øvrebekk¹⁴, J. Vrláková³⁴, B. Vulpescu⁶³, A. Vyushin⁸⁷, B. Wagner¹⁴, V. Wagner³³, R. Wan^{58,39}, D. Wang³⁹, M. Wang³⁹, Y. Wang⁸², Y. Wang³⁹, K. Watanabe¹¹⁴, J.P. Wessels^{29,54}, U. Westerhoff⁵⁴, J. Wiechula¹¹⁵, J. Wikne¹⁷, M. Wilde⁵⁴, G. Wilk¹⁰⁰, A. Wilk⁵⁴, M.C.S. Williams⁹⁷, B. Windelband⁸², L. Xaplanteris Karampatsos¹⁰⁵, H. Yang¹¹, S. Yang¹⁴, S. Yasnopolskiy⁸⁸, J. Yi⁸⁴, Z. Yin³⁹, H. Yokoyama¹¹⁴, I.-K. Yoo⁸⁴, J. Yoon¹²³, W. Yu⁵², X. Yuan³⁹, I. Yushmanov⁸⁸, C. Zach³³, C. Zampolli^{97,29}, S. Zaporozhets⁵⁹, A. Zarochentsev¹¹⁷, P. Závada⁴⁹, N. Zaviyalov⁸⁷, H. Zbroszczyk¹¹⁸, P. Zelniczek⁵¹, I.S. Zgura⁵⁰, M. Zhalov⁷⁵, X. Zhang^{63,39}, Y. Zhou⁴⁵, D. Zhou³⁹, F. Zhou³⁹, X. Zhu³⁹, A. Zichichi^{21,9}, A. Zimmermann⁸², G. Zinovjev², Y. Zoccarato¹⁰⁹, M. Zynovyev²

¹ Benemérita Universidad Autónoma de Puebla, Puebla, Mexico

² Bogolyubov Institute for Theoretical Physics, Kiev, Ukraine

³ Budker Institute for Nuclear Physics, Novosibirsk, Russia

⁴ California Polytechnic State University, San Luis Obispo, CA, United States

⁵ Centre de Calcul de l'IN2P3, Villeurbanne, France

⁶ Centro de Aplicaciones Tecnológicas y Desarrollo Nuclear (CEADEN), Havana, Cuba

⁷ Centro de Investigaciones Energéticas Medioambientales y Tecnológicas (CIEMAT), Madrid, Spain

⁸ Centro de Investigación y de Estudios Avanzados (CINVESTAV), Mexico City and Mérida, Mexico

⁹ Centro Fermi – Centro Studi e Ricerche e Museo Storico della Fisica “Enrico Fermi”, Rome, Italy

¹⁰ Chicago State University, Chicago, IL, United States

¹¹ Commissariat à l’Energie Atomique, IRFU, Saclay, France

¹² Departamento de Física de Partículas and IGFAE, Universidad de Santiago de Compostela, Santiago de Compostela, Spain

¹³ Department of Physics, Aligarh Muslim University, Aligarh, India

¹⁴ Department of Physics and Technology, University of Bergen, Bergen, Norway

¹⁵ Department of Physics, Ohio State University, Columbus, OH, United States

¹⁶ Department of Physics, Sejong University, Seoul, South Korea

¹⁷ Department of Physics, University of Oslo, Oslo, Norway

¹⁸ Dipartimento di Fisica dell’Università and Sezione INFN, Cagliari, Italy

¹⁹ Dipartimento di Fisica dell’Università and Sezione INFN, Padova, Italy

²⁰ Dipartimento di Fisica dell’Università and Sezione INFN, Trieste, Italy

²¹ Dipartimento di Fisica dell’Università and Sezione INFN, Bologna, Italy

²² Dipartimento di Fisica dell’Università ‘La Sapienza’ and Sezione INFN, Rome, Italy

²³ Dipartimento di Fisica e Astronomia dell’Università and Sezione INFN, Catania, Italy

²⁴ Dipartimento di Fisica ‘E.R. Caianiello’ dell’Università and Gruppo Collegato INFN, Salerno, Italy

²⁵ Dipartimento di Fisica Sperimentale dell’Università and Sezione INFN, Turin, Italy

²⁶ Dipartimento di Scienze e Tecnologie Avanzate dell’Università del Piemonte Orientale and Gruppo Collegato INFN, Alessandria, Italy

²⁷ Dipartimento Interateneo di Fisica ‘M. Merlin’ and Sezione INFN, Bari, Italy

²⁸ Division of Experimental High Energy Physics, University of Lund, Lund, Sweden

²⁹ European Organization for Nuclear Research (CERN), Geneva, Switzerland

³⁰ Fachhochschule Köln, Köln, Germany

³¹ Faculty of Engineering, Bergen University College, Bergen, Norway

- ³² Faculty of Mathematics, Physics and Informatics, Comenius University, Bratislava, Slovakia
- ³³ Faculty of Nuclear Sciences and Physical Engineering, Czech Technical University in Prague, Prague, Czech Republic
- ³⁴ Faculty of Science, P.J. Šafárik University, Košice, Slovakia
- ³⁵ Frankfurt Institute for Advanced Studies, Johann Wolfgang Goethe-Universität Frankfurt, Frankfurt, Germany
- ³⁶ Gangneung-Wonju National University, Gangneung, South Korea
- ³⁷ Helsinki Institute of Physics (HIP) and University of Jyväskylä, Jyväskylä, Finland
- ³⁸ Hiroshima University, Hiroshima, Japan
- ³⁹ Hua-Zhong Normal University, Wuhan, China
- ⁴⁰ Indian Institute of Technology, Mumbai, India
- ⁴¹ Indian Institute of Technology Indore (IIT), Indore, India
- ⁴² Institut de Physique Nucléaire d'Orsay (IPNO), Université Paris-Sud, CNRS-IN2P3, Orsay, France
- ⁴³ Institute for High Energy Physics, Protvino, Russia
- ⁴⁴ Institute for Nuclear Research, Academy of Sciences, Moscow, Russia
- ⁴⁵ Nikhef, National Institute for Subatomic Physics and Institute for Subatomic Physics of Utrecht University, Utrecht, Netherlands
- ⁴⁶ Institute for Theoretical and Experimental Physics, Moscow, Russia
- ⁴⁷ Institute of Experimental Physics, Slovak Academy of Sciences, Košice, Slovakia
- ⁴⁸ Institute of Physics, Bhubaneswar, India
- ⁴⁹ Institute of Physics, Academy of Sciences of the Czech Republic, Prague, Czech Republic
- ⁵⁰ Institute of Space Sciences (ISS), Bucharest, Romania
- ⁵¹ Institut für Informatik, Johann Wolfgang Goethe-Universität Frankfurt, Frankfurt, Germany
- ⁵² Institut für Kernphysik, Johann Wolfgang Goethe-Universität Frankfurt, Frankfurt, Germany
- ⁵³ Institut für Kernphysik, Technische Universität Darmstadt, Darmstadt, Germany
- ⁵⁴ Institut für Kernphysik, Westfälische Wilhelms-Universität Münster, Münster, Germany
- ⁵⁵ Instituto de Ciencias Nucleares, Universidad Nacional Autónoma de México, Mexico City, Mexico
- ⁵⁶ Instituto de Física, Universidad Nacional Autónoma de México, Mexico City, Mexico
- ⁵⁷ Institut of Theoretical Physics, University of Wrocław, Poland
- ⁵⁸ Institut Pluridisciplinaire Hubert Curien (IPHC), Université de Strasbourg, CNRS-IN2P3, Strasbourg, France
- ⁵⁹ Joint Institute for Nuclear Research (JINR), Dubna, Russia
- ⁶⁰ KFKI Research Institute for Particle and Nuclear Physics, Hungarian Academy of Sciences, Budapest, Hungary
- ⁶¹ Kirchhoff-Institut für Physik, Ruprecht-Karls-Universität Heidelberg, Heidelberg, Germany
- ⁶² Korea Institute of Science and Technology Information, South Korea
- ⁶³ Laboratoire de Physique Corpusculaire (LPC), Clermont Université, Université Blaise Pascal, CNRS-IN2P3, Clermont-Ferrand, France
- ⁶⁴ Laboratoire de Physique Subatomique et de Cosmologie (LPSC), Université Joseph Fourier, CNRS-IN2P3, Institut Polytechnique de Grenoble, Grenoble, France
- ⁶⁵ Laboratori Nazionali di Frascati, INFN, Frascati, Italy
- ⁶⁶ Laboratori Nazionali di Legnaro, INFN, Legnaro, Italy
- ⁶⁷ Lawrence Berkeley National Laboratory, Berkeley, CA, United States
- ⁶⁸ Lawrence Livermore National Laboratory, Livermore, CA, United States
- ⁶⁹ Moscow Engineering Physics Institute, Moscow, Russia
- ⁷⁰ National Institute for Physics and Nuclear Engineering, Bucharest, Romania
- ⁷¹ Niels Bohr Institute, University of Copenhagen, Copenhagen, Denmark
- ⁷² Nikhef, National Institute for Subatomic Physics, Amsterdam, Netherlands
- ⁷³ Nuclear Physics Institute, Academy of Sciences of the Czech Republic, Řež u Prahy, Czech Republic
- ⁷⁴ Oak Ridge National Laboratory, Oak Ridge, TN, United States
- ⁷⁵ Petersburg Nuclear Physics Institute, Gatchina, Russia
- ⁷⁶ Physics Department, Creighton University, Omaha, NE, United States
- ⁷⁷ Physics Department, Panjab University, Chandigarh, India
- ⁷⁸ Physics Department, University of Athens, Athens, Greece
- ⁷⁹ Physics Department, University of Cape Town, iThemba LABS, Cape Town, South Africa
- ⁸⁰ Physics Department, University of Jammu, Jammu, India
- ⁸¹ Physics Department, University of Rajasthan, Jaipur, India
- ⁸² Physikalisches Institut, Ruprecht-Karls-Universität Heidelberg, Heidelberg, Germany
- ⁸³ Purdue University, West Lafayette, IN, United States
- ⁸⁴ Pusan National University, Pusan, South Korea
- ⁸⁵ Research Division and ExtreMe Matter Institute EMMI, GSI Helmholtzzentrum für Schwerionenforschung, Darmstadt, Germany
- ⁸⁶ Rudjer Bošković Institute, Zagreb, Croatia
- ⁸⁷ Russian Federal Nuclear Center (VNIIEF), Sarov, Russia
- ⁸⁸ Russian Research Centre Kurchatov Institute, Moscow, Russia
- ⁸⁹ Saha Institute of Nuclear Physics, Kolkata, India
- ⁹⁰ School of Physics and Astronomy, University of Birmingham, Birmingham, United Kingdom
- ⁹¹ Sección Física, Departamento de Ciencias, Pontificia Universidad Católica del Perú, Lima, Peru
- ⁹² Sezione INFN, Trieste, Italy
- ⁹³ Sezione INFN, Padova, Italy
- ⁹⁴ Sezione INFN, Turin, Italy
- ⁹⁵ Sezione INFN, Rome, Italy
- ⁹⁶ Sezione INFN, Cagliari, Italy
- ⁹⁷ Sezione INFN, Bologna, Italy
- ⁹⁸ Sezione INFN, Bari, Italy
- ⁹⁹ Sezione INFN, Catania, Italy
- ¹⁰⁰ Soltan Institute for Nuclear Studies, Warsaw, Poland
- ¹⁰¹ Nuclear Physics Group, STFC Daresbury Laboratory, Daresbury, United Kingdom
- ¹⁰² SUBATECH, Ecole des Mines de Nantes, Université de Nantes, CNRS-IN2P3, Nantes, France
- ¹⁰³ Technical University of Split FESB, Split, Croatia
- ¹⁰⁴ The Henryk Niewodniczanski Institute of Nuclear Physics, Polish Academy of Sciences, Cracow, Poland
- ¹⁰⁵ The University of Texas at Austin, Physics Department, Austin, TX, United States
- ¹⁰⁶ Universidad Autónoma de Sinaloa, Culiacán, Mexico
- ¹⁰⁷ Universidade de São Paulo (USP), São Paulo, Brazil
- ¹⁰⁸ Universidade Estadual de Campinas (UNICAMP), Campinas, Brazil
- ¹⁰⁹ Université de Lyon, Université Lyon 1, CNRS/IN2P3, IPN-Lyon, Villeurbanne, France
- ¹¹⁰ University of Houston, Houston, TX, United States

¹¹¹ University of Technology and Austrian Academy of Sciences, Vienna, Austria

¹¹² University of Tennessee, Knoxville, TN, United States

¹¹³ University of Tokyo, Tokyo, Japan

¹¹⁴ University of Tsukuba, Tsukuba, Japan

¹¹⁵ Eberhard Karls Universität Tübingen, Tübingen, Germany

¹¹⁶ Variable Energy Cyclotron Centre, Kolkata, India

¹¹⁷ V. Fock Institute for Physics, St. Petersburg State University, St. Petersburg, Russia

¹¹⁸ Warsaw University of Technology, Warsaw, Poland

¹¹⁹ Wayne State University, Detroit, Michigan, United States

¹²⁰ Yale University, New Haven, CT, United States

¹²¹ Yerevan Physics Institute, Yerevan, Armenia

¹²² Yildiz Technical University, Istanbul, Turkey

¹²³ Yonsei University, Seoul, South Korea

¹²⁴ Zentrum für Technologietransfer und Telekommunikation (ZTT), Fachhochschule Worms, Worms, Germany

* Corresponding author.

E-mail address: blume@ikf.uni-frankfurt.de (C. Blume).

ⁱ Also at: M.V. Lomonosov Moscow State University, D.V. Skobeltsyn Institute of Nuclear Physics, Moscow, Russia.

ⁱⁱ Also at: “Vinča” Institute of Nuclear Sciences, Belgrade, Serbia.